The Kautsky Curve Is a Built-in Barcode

Esa Tyystjärvi,* Antti Koski,# Mika Keränen,* and Olli Nevalainen#
*University of Turku, Department of Biology, Laboratory of Plant Physiology, BioCity A, and #University of Turku, Department of Computer Science, DataCity, FIN-20014 Turku, Finland

ABSTRACT We identify objects from their visually observable morphological features. Automatic methods for identifying living objects are often needed in new technology, and these methods try to utilize shapes. When it comes to identifying plant species automatically, machine vision is difficult to implement because the shapes of different plants overlap and vary greatly because of different viewing angles in field conditions. In the present study we show that chlorophyll *a* fluorescence, emitted by plant leaves, carries information that can be used for the identification of plant species. Transient changes in fluorescence intensity when a light is turned on were parameterized and then subjected to a variety of pattern recognition procedures. A Self-Organizing Map constructed from the fluorescence signals was found to group the signals according to the phylogenetic origins of the plants. We then used three different methods of pattern recognition, of which the Bayesian Minimum Distance classifier is a parametric technique, whereas the Multilayer Perceptron neural network and *k*-Nearest Neighbor techniques are nonparametric. Of these techniques, the neural network turned out to be the most powerful one for identifying individual species or groups of species from their fluorescence transients. The excellent recognition accuracy, generally over 95%, allows us to speculate that the method can be further developed into an application in precision agriculture as a means of automatically identifying plant species in the field.

INTRODUCTION

Most of the light absorbed by a plant leaf is utilized by photosynthesis or converted into heat, but a small proportion, a few percent of the absorbed light at most, is reemitted as chlorophyll *a* fluorescence. The photochemical reaction of photosynthesis and emission of fluorescence compete for the same absorbed quanta—the more photochemistry, the less fluorescence. Because of this complementarity, chlorophyll fluorescence is a built-in probe of photosynthesis, and indeed fluorescence is a popular method in plant physiology (see reviews by Krause and Weis, 1991; Govindjee, 1995). The current pulse amplitude modulation technique (Schreiber et al., 1986) allows changes in chlorophyll *a* fluorescence yield to be measured from leaves in field conditions. In this technique, a dim blinking beam of light is used to excite fluorescence, and all continuous reflected light is filtered from the signal.

The most widely used fluorescence technique is fluorescence induction or measurement of changes in fluorescence yield when a light is abruptly switched on after a dark period. When a light is switched on, the fluorescence yield rapidly rises and then slowly decreases (Fig. 1). This fluorescence induction has been termed the *Kautsky phenomenon*, after its discoverer (Kautsky and Hirsch, 1931). Most chlorophyll *a* fluorescence is emitted by photosystem II (PSII), which extracts electrons from water and feeds them to the electron transfer chain connecting the two photosystems. When a light is switched on, photosystem II transiently reduces its electron acceptor quinone Q_A, and the reduction is reflected by a transient increase in the fluorescence yield.

The Kautsky phenomenon has been found to be extremely suitable for the screening of physiological parameters of plants. Photoinhibition of photosynthesis (Aro et al., 1993), herbicide effects (Shaw et al., 1985), cold acclimation (Lindgren and Hällgren, 1993), and effects of air pollution (Schreiber et al., 1978) are examples of physiological responses in which one numerical parameter of the fluorescence curve, often the ratio of so-called variable fluorescence (maximum minus initial fluorescence) to maximum fluorescence ($(F_{MAX} - F_0)/F_{MAX}$; see Fig. 1), has been successfully used as an indicator of the physiological state of a plant.

The kinetics of the transient closure of photosystem II reaction centers and the exact pattern of increase and subsequent decrease in the fluorescence yield depend on several structural and functional features of the plant. For example, the rate of increase in the fluorescence yield during the closure of PSII centers depends on the size of the light-harvesting antenna, because the frequency of primary charge separations is proportional to the product of light intensity and the amount of light-harvesting chlorophyll. On the other hand, the rate of increase in the fluorescence yield also depends on the size and reduction state of the plastoquinone pool connecting the two photosystems because the plastoquinone pool oxidizes the Q_A electon acceptor. Several other factors affect the fluorescence transient, e.g., the efficiency of excitation energy transfer among PSII units (connectivity), the state of the oxygen evolving complex, the rate of plastoquinone oxidation, and various nonphotochemical phenomena that quench fluorescence (for simu-

Received for publication 4 March 1999 and in final form 26 April 1999.
Address reprint requests to Dr. Esa Tyystjärvi, University of Turku, Department of Biology, Laboratory of Plant Physiology, Biocity A, FIN-20014 Turku, Finland. Tel.: +358-2-3338079; Fax: +358-2-3338075; E-mail: esatyy@utu.fi.

0006-3495/99/08/1159/09 $2.00

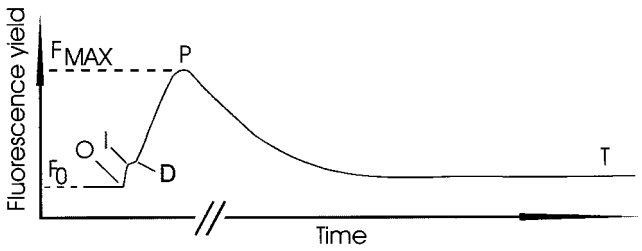

FIGURE 1 Schematic overview of the Kautsky curve. The yield of chlorophyll *a* fluorescence is high when the quinone electron acceptor Q_A of PSII is reduced, and low when it is oxidized. A sudden increase in light intensity results in a transient accumulation of Q_A^-, which is reflected as a transient increase in the fluorescence yield. Fluorescence yield is also affected by nonphotochemical quenching phenomena. O (F_0 level), I, D, P (if all Q_A is reduced, P peak is at F_{MAX} level), and T are conventional names for the indicated points of the Kautsky curve.

lated effects of a number of different factors, see Stirbet et al., 1998).

The basic pattern of the Kautsky curve is similar in all plants (Fig. 1). It consists of a rapid increase to a F_0 level, followed by a multiphasic rise toward a peak value (F_P) and then a multiphasic decay to a constant terminal level (F_T). A linear plot shows one plateau, characterized by the turnpoints I and D (Fig. 1). Plotting the same data with a logarithmic time scale would also reveal a "J" wave between O and I (Strasser et al., 1995; Stirbet et al., 1998).

The constancy of the pattern of the Kautsky curve renders it suitable for pattern recognition. In the present study, we show that although the pattern is similar in all plants, species-specific differences are so large that they allow the curve, the "fluorescence fingerprint," to be used to identify plants.

Pattern recognition methods can be applied to unsupervised learning to find natural clusters of the data (Jain, 1988). We first illustrated the natural grouping of fluorescence curves by creating a *Self-Organizing Map* (SOM) (Kohonen, 1990), which implements a mapping from the space of input parameters to a grid of reference vectors in such a way that the grid visualizes the density function of the input data. Examination of the SOM reveals whether the natural clusters coincide with the known clusters of the data.

A *neural network* is one of the most popular automatic discriminant generation methods used in pattern recognition (Chen and Titterington, 1994; Schalkoff, 1992; Rich and Knight, 1991). Neural networks are rule-learning systems with highly parallel and simple architecture. Among the many possible variants, the Multilayer Perceptron neural network (MLP) with the error back-propagation training rule has been successfully applied in biomedical signal analysis. The MLP is a nonparametric classifier requiring a training set of samples with known classification. The network is optimized to this training set and its power is evaluated against an independent test set. The MLP is a supervised neural network, which means that we must have a prior knowledge of the class membership for the members of the representative training set.

In addition to the MLP, we applied two other common statistical pattern recognition methods (Cohen, 1988; Schalkoff, 1992). The *Bayesian Minimum Distance* (BMD) classification is a parametric method that minimizes the mean square error of the class quantization. If we can assume that the class density functions are Gaussian with equal class probabilities and uncorrelated features with equal variances, we may estimate the class centroids and classify each object according to the nearest centroid. BMD can only be applied to clusters of multinormal form, which restricts its applicability in complex situations.

As the fourth technique we used the *k-Nearest Neighbor* (*k*-NN) classifier. In this nonparametric classification we suppose that we know the class membership of the samples in a training set. The classification of an unknown sample is done by voting: a new sample is compared with the known samples, and its distance to each of them is calculated. A sample is classified to the cluster to which the majority of its *k* nearest neighbors belong. For avoiding ties it is natural to use odd *k* values (typically from 5 to 9).

Although our current application of fluorescence fingerprinting is far from being suitable for field use, we are confident that the method can be developed into a useful tool for automatic identification of plants in precision farming (Blackmore, 1994).

MATERIALS AND METHODS

Two sets of data were collected. In the first set of experiments (8-s data), the following plant species were used: Scotch pine (*Pinus sylvatica* L.), Norwegian spruce (*Picea abies* L.), dandelion (*Taraxacum officinale* L.), birch (*Betula pendula* L.), pea (*Pisum sativum* L.), pumpkin (*Cucurbita pepo* L. cv Jättiläismeloni), and rye (*Secale cereale* L. cv Voima). Dandelion, birch, pine, and spruce leaves were collected from a local park, and pumpkin, pea, and rye were grown under controlled conditions in a phytotron (20°C, 12-h day/night cycle, 300–500 μmol photons m^{-2} s^{-1}, 60% relative humidity). In the second set of experiments (3-s data), we used Scotch pine (collected from the park); birch (from the park); two batches of rye (one batch grown in a phytotron and one grown in a greenhouse); couch grass (*Elytrigia repens*, grown in a greenhouse); tobacco (*Nicotiana tabacum* L., grown in a phytotron); mosses *Sphagnum fuscum* and *Polytrichum commune*, both collected from a forest; and lichen (*Hylocomnium physodes*, collected from a forest). In the case of *Hylocomnium*, its symbiontic green alga is the fluorescence-emitting species.

The leaves were stored in the dark between moist paper towels for ~2 h before the measurement of chlorophyll fluorescence induction. Two hundred measurements were made on each species. Each measurement of *Taraxacum*, *Pisum*, and *Betula* was made on a separate leaf, and bunches of 10–20 pine and spruce needles were used. Twenty pumpkin leaves were cut into 10 pieces each, and three sections from 67 rye leaves were used to obtain 200 curves. In the 8-s experiment, pumpkin, birch, pea, and rye data were collected separately from both sides of the leaf, and the upper and lower sides of the leaf were treated as two separate classes, and dandelion was measured from the upper leaf surface only. The 3-s data were collected from the adaxial sides of birch, rye, couch grass, and tobacco leaves; from bunches of pine needles and moss leaves; and from the surface of the thallus of the lichen.

Fluorescence was measured with a pulse amplitude modulation fluorometer (PAM 101; Heinz Walz GmbH, Effeltrich, Germany) equipped with a red LED illuminator (PAM-102L), a far-red LED (PAM-102FR), and a saturation pulse lamp (KL-1500). The different illumination phases of the 8-s and 3-s experiments are described in Fig. 2, *A* and *D*, respec-

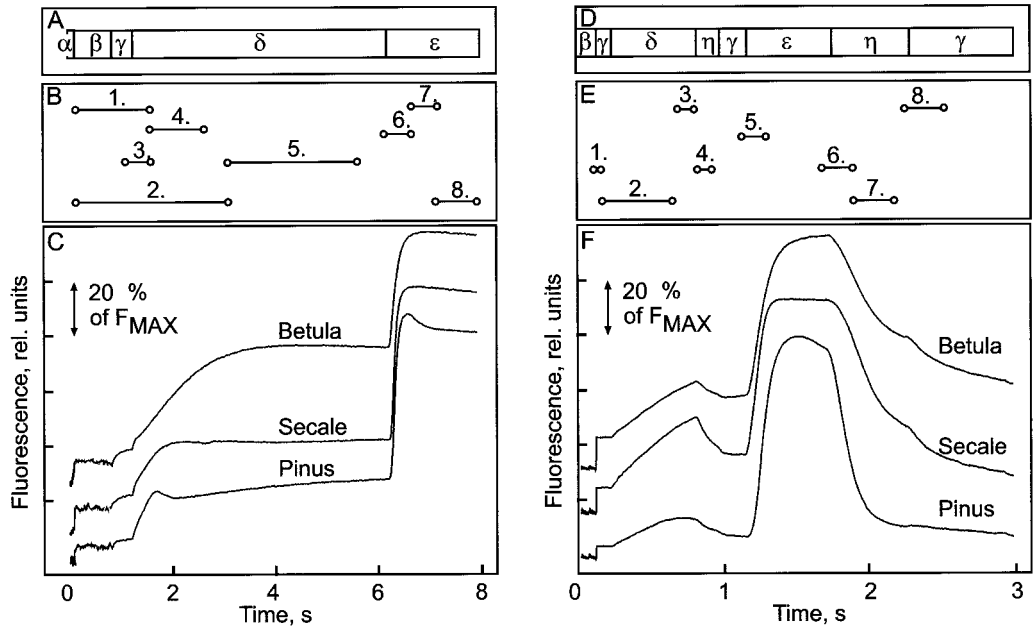

FIGURE 2 Illumination phases used to obtain the fluorescence induction traces (*A*, *D*); the positions of regression line segments used for the parameterization of the data (*B*, *E*); and individual fluorescence induction curves measured from birch, rye, and pine (*C*, *F*) in the 8-s (*A–C*) and the 3-s (*D–F*) experiments. (*A*, *D*) Illumination phases, labeled as follows: α, Trigger phase during which a leaf was gently pressed to the probe of the fluorometer. The increase in the fluorescence yield informs the software that a leaf has been brought to the focus of the fluorometer. This phase was removed before analysis and is shown for the 8-s experiment only. β, F_0 phase, during which the measuring beam of the fluorometer was set to operate at 1.6 kHz blinking frequency. γ, Phase during which the measuring beam of the fluorometer was blinking at 100 kHz but the sample was otherwise in the dark. δ, Low actinic light phase after a red LED illuminator is switched on (60 μmol photons m^{-2} s^{-1}). η, Far red light (735 nm) illumination. ϵ, F_{MAX} phase when a high-intensity white light is switched on (5500 μmol photons m^{-2} s^{-1}). (*B*, *E*) The start and end points of the regression lines used in the pattern recognition procedure (numbered 1–8). (*C*, *F*) Fluorescence transients of three species. The curves are shifted in the *y* axis direction to facilitate comparison. To test the 1-s curves, we used the first part of the data from 0 to 1 s in *F*.

tively. Each curve was recorded with a resolution of 12 bits, and 1600 sample points from each curve were used for the analysis. The fluorometer was controlled and the data were digitized with the FIP software (QA-DATA OY, Turku, Finland). The PAM-101 fluorometer was modified slightly to allow the red LED and the FR LED to be switched on and off in the control of the computer.

The fluorescence signals were normalized before extraction of the parameters in the range [0, 1]. Eight regression lines (positions shown in Fig. 2 *B* for the 8-s experiment and in Fig. 2 *E* for the 3-s experiment) were then calculated, and the corresponding 16 coefficients were normalized into the range [0, 1]. We used both the slopes and *y* axis intercepts of the regression lines to obtain a more accurate description of the data and to avoid too high weights of single features. These coefficients serve as a 16-dimensional feature vector representing each sample signal. Because the time limits of the line segments were fixed by the experimental protocol used to measure the fluorescence signal, there was no need for more complicated analysis methods used for time-varying signals (Fu, 1982).

A SOM is a general projection from the multidimensional feature space into a more visual two-dimensional form. The SOM was created in a standard way (Kohonen, 1990; Kohonen et al., 1995) by starting from a set of arbitrary reference vectors projecting the input space to the map plane. The reference vectors are organized as a two-dimensional *neighborhood matrix*, and Euclidean distances between the input vectors and the nodes of the map are calculated. The SOM is trained in an iterative process in which we pick up an input vector and locate the best-matching reference vector **R** for this feature vector. This reference vector **R** and its *neighbor vectors* (i.e., other reference vectors located inside a predetermined *neighborhood radius* on the neighborhood matrix) are updated so that they map vectors of the input space closer to the reference vector **R**. The neighborhood radius and the factor by which the reference vectors are changed in each training step are reduced during the process. The result of the process is an organization that obeys the density function of the input data. The map distributes its reference vectors into the multidimensional input space, so that similar reference vectors lie near each other in the neighborhood grid. The density of the training vectors can be visualized by the darkness of the background of the map, with light areas indicating dense areas of the training set.

In the subsequent pattern recognition experiments, the training set consisted of 1000 curves (10 separate pattern classes and 100 training curves from each class), and the remaining 1000 curves (100 curves from each class, or 99 curves in the 3-s experiment) were used to test the power of the technique. The training and test cases were randomly selected from the 200 curves measured from each species.

We used the MLP neural network approach (Schalkoff, 1992) as the primary tool for identifying the fluorescence fingerprints. The MLP implements a mapping from the *N* input elements ($X_1, \ldots, X_N$) to the output elements ($O_1, \ldots, O_K$) through the *M* elements ($H_1, \ldots, H_M$) of the so-called hidden layer (Fig. 3 *A*). The mapping is done by the weights assigned to each link between each two nodes in two consecutive layers. Each node computes the weighted sum of its inputs and uses a sigmoid output function (Eqs. 1–2) to calculate its output, as follows:

$$H_j = \frac{1}{1 + \exp(-\sum_{i=0}^{N} W1_{ij} X_i)}, \quad j = 1..M; \quad X_0 = 1 \qquad (1)$$

and

$$O_j = \frac{1}{1 + \exp(-\sum_{i=0}^{M} W2_{ij} H_i)}, \quad j = 1..K; \quad H_0 = 1. \qquad (2)$$

There are as many output cells as there are pattern classes, and in the ideal case, the optimum output value is 1 for the correct class and 0 for all

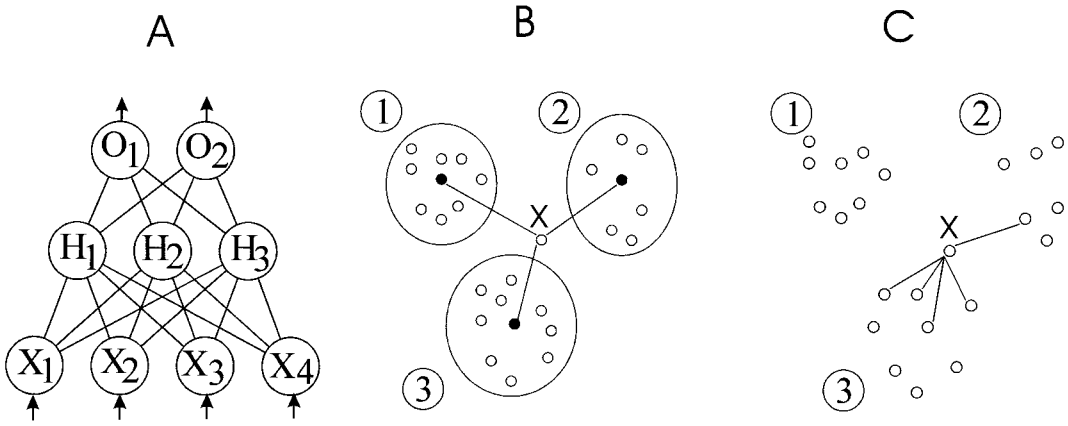

FIGURE 3 Schematic representations of the architecture of three pattern recognition techniques. (*A*) An MLP consisting of four input cells $X_1 \ldots X_4$, three cells $H_1 \ldots H_3$ of the hidden layer, and two output cells, O_1 and O_2. The MLPs used in this study consisted of 14–16 input cells, 14–21 cells of the hidden layer, and 8–10 output cells, as indicated. (*B*) A BMD classifier showing centroids of three clusters. An unknown signal X is classified to cluster 3 because its distance from the mean of this cluster is shortest. (*C*) A 5-NN classifier. An unknown sample X is classified to cluster 3 because four of its five nearest neighbors belong therein. In the present study we used a 9-NN classifier.

other classes. When using a trained MLP, each output O_i may take any value between 0 and 1, and the sample is classified to the class with the highest output value.

The connection weights are adjusted according to the back-propagation rule, which is a gradient-descending optimization technique aimed at minimizing the mean square error of the output in comparison to the a priori classification of the training vectors. In each optimization step, the weights $W2_{ij}$ and $W1_{ls}$ ($i = 0..M$; $j = 1..K$; $l = 0..N$; $s = 1..M$) are changed as follows:

$$\Delta W2_{ij} = \eta O_j(1 - O_j)(Y_j - O_j)H_i, \quad i = 0..M; \quad j = 1..K \tag{3}$$

and

$$\Delta W1_{ls} = \eta H_s(1 - H_s)\left(\sum_{k=1}^{K} O_k(1 - O_k)(Y_k - O_k)W2_{sk}\right)X_l, \quad l = 0..N; \quad s = 1..M. \tag{4}$$

In Eqs. 3 and 4, Y_k is the correct output value (either 0 or 1), and O_k is the corresponding MLP output value. The constant η is the *learning rate* of the MLP network, usually in the range of 0.01–0.05. The speed and convergence of this basic back-propagation algorithm can be enhanced by several methods (Rich and Knight, 1991). MLP reaches a local minimum of the error function by repeating the back-propagation training sufficiently many times. Fig. 3 *A* shows schematically the architecture of the MLP used for the fluorescence fingerprints. The simple structure of the network gives us a short recognition time, but the training can be time-consuming. Only a small amount of memory is needed to store the network.

An MLP can also be realized by a geometrical interpretation. Each node of the hidden layer determines discriminating hyperplanes in the feature space, and each node of the output layer collects a group of these planes to form a complex shaped area containing a certain class of patterns.

The MLP used in the 8-s experiment consisted of 16 inputs, corresponding to the 16 features, and 10 outputs (corresponding to 10 classes) interconnected by 14 intermediate nodes; in the 3-s experiment we used 16 inputs, 21 intermediate nodes, and 10 outputs. The number of hidden nodes is an adjustable parameter. If the pattern classes are very complicated in shape, then a high number of hidden nodes may help to obtain a good recognition accuracy. On the other hand, if the network contains too many hidden nodes, it may overlearn to recognize the noise of the training set. In general, the number of hidden nodes should be just large enough for a good recognition of the test set. In practical applications the number of hidden nodes is usually nearly the same as the number of input and output nodes.

The network was trained with 4000 iterations of the back-propagation algorithm to identify the classes correctly. We also tested for shortening of the signal by taking only the first second of the 3-s experiment into the analysis; in this case the MLP consisted of 14 inputs, 10 outputs, and 21 intermediate nodes.

As a rule of thumb, an MLP teaching set is usually sized several times larger than the number of connection weights ($16 \times 14 \times 10 = 2240$ weights in the case of the 8-s experiment). We decided to use a moderate teaching set consisting of 1000 events for these first experiments to be able to collect or cultivate the plants and test the method with a high number of species.

Additional pattern recognition tests were done with the BMD and *k*-NN classifiers. In the BMD classifier we calculate the arithmetic mean (i.e., centroid) of the feature vectors of each signal class. The feature vectors of the test set are then classified to the class for which the cluster centroid is closest to the test vector (Fig. 3 *B*). The distances were calculated using conventional Euclidean metrics. The Euclidean distance depends heavily on the feature scale, but because our features were normalized to the range [0, 1], each feature had an equal effect on the distance. In the BMD classification we need to store only the centroid vectors, and the classification is extremely rapid.

The *k*-NN classifier can be regarded as a nonparametric generalization of the BMD method, and it can be used without any knowledge of the class probability functions of the training set. In the *k*-NN classification we must store all of the training vectors, calculate the distance of an unknown signal from each of them, and finally find the *k* shortest distances (Fig. 3 *C*), which may be quite time-consuming.

RESULTS

Self-Organizing Map

Fig. 4 shows the 16×10 SOM constructed from the 3-s experiment; the SOM of the 8-s experiment (not shown) would bring us to the same conclusions. Three important features are apparent in the SOM. First, most fluorescence curves belong to well-organized clusters representing a plant species. Some clusters are somewhat broken up, indi-

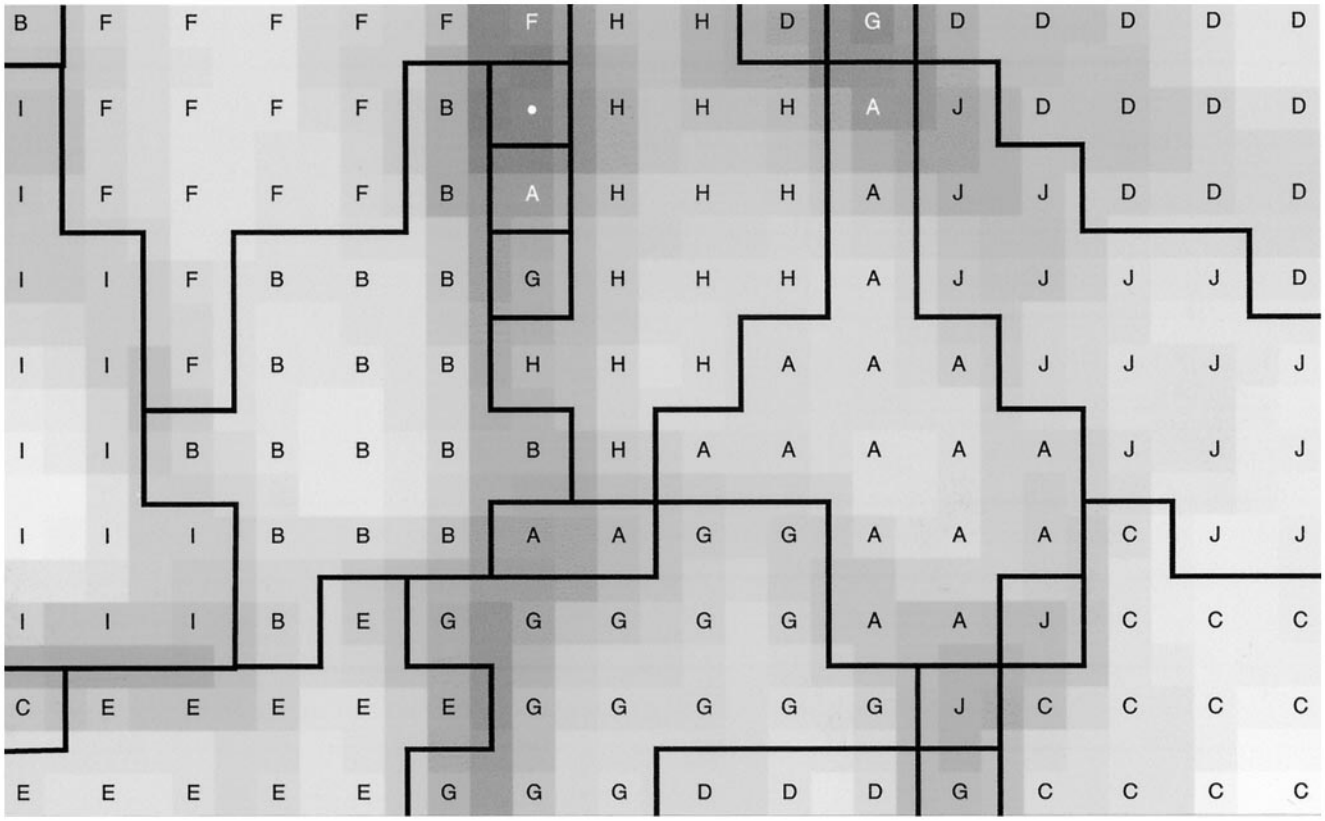

FIGURE 4 SOM of the 3-s experiment. All 10 × 200 feature vectors were used to create the map. The reference vectors are organized in a regular matrix. The dark areas indicate long Euclidean distances between two adjacent reference vectors. Each node is labeled by the code letter indicating the species to which the majority of the reference vectors of the node belong. The different species are coded as follows: A, *Elytrigia*; B, *Polytrichum*; C, *Betula*; D, *Zea*; E, *Pinus*; F, *Sphagnum*; G, *Secale* (grown in a phytotron); H, *Secale* (grown in a greenhouse); I, *Hypogymnium*; J, *Nicotiana*. The lines illustrate the clusters.

cating that the similarity-based clustering of the data is not perfect. Second, as expected, not only the species but also growth conditions affect the shape of the curve, and therefore rye plants grown in two culture conditions fall into two clusters: phytotron rye and greenhouse rye. Third, the fluorescence curves of the higher plants form a cluster that is clearly separated from the gymnosperm cluster (pine, mosses, and the green alga partner of the lichen). The well-organized clusterization of the data and the coincidence of the similarity-based clusters with the plant species promised a high accuracy of recognition of the plant species with pattern recognition tools.

TABLE 1 Recognition matrix of the 8-s experiment

	Recognized as									
Species	*Betula* (u)	*Betula* (l)	*Cucurbita* (u)	*Cucurbita* (l)	*Picea*	*Pisum* (u)	*Pisum* (l)	*Pinus*	*Secale*	*Taraxacum*
Betula (u)	96	3	0	0	0	0	0	0	1	0
Betula (l)	0	97	0	1	0	0	0	0	0	3
Cucurbita (u)	1	0	98	0	0	0	1	0	0	0
Cucurbita (l)	0	1	0	97	0	0	0	0	1	1
Picea	0	1	0	0	98	0	1	0	0	0
Pisum (u)	0	0	0	0	0	93	7	0	0	0
Pisum (l)	0	0	0	3	0	1	95	0	1	0
Pinus	0	0	0	0	1	0	0	99	0	0
Secale	0	0	0	0	1	0	2	0	97	0
Taraxacum	0	4	0	0	0	0	0	0	0	96

The identification was done with a neural network algorithm, using the slope and *y* axis intercept of eight normalized regression lines calculated from different partly overlapping sections of each curve (see Fig. 2 *B* for the start and end points of the regression line segments). The adaxial or upper (u) and abaxial or lower (l) sides of the leaf were treated as separate classes in *Betula*, *Cucurbita*, and *Pisum*. *Betula*, *Picea*, *Pinus*, and *Taraxacum* were collected from outside, and *Cucurbita*, *Pisum*, and *Secale* were grown under controlled conditions in a phytotron.

TABLE 2 Recognition matrix of the 3-s experiment, using a MLP neural network for the identification

	Recognized as									
Species	*Betula* (o)	*Nicotiana* (p)	*Zea* (p)	*Secale* (p)	*Secale* (g)	*Elytrigia* (g)	*Pinus* (o)	*Polytrichum* (o)	*Sphagnum* (o)	*Hylocomnium* (o)
Betula (o)	96	2	1	0	0	0	0	0	0	0
Nicotiana (p)	2	97	0	0	0	0	0	0	0	0
Zea (p)	0	1	88	9	0	0	0	0	0	0
Secale (p)	0	3	6	88	1	1	0	0	0	0
Secale (g)	0	0	0	0	98	1	0	0	0	0
Elytrigia (g)	0	0	0	0	0	99	0	0	0	0
Pinus (o)	0	0	0	0	0	0	99	0	0	0
Polytrichum (o)	0	0	0	0	0	0	0	96	2	1
Sphagnum (o)	0	0	0	0	1	0	0	6	91	1
Hylocomnium (o)	0	0	0	0	1	0	0	1	0	97

Each curve was characterized by the slope and *y* axis intercept of eight normalized regression lines calculated from different partly overlapping sections of the curve (see Fig. 2 *E* for the positions). The adaxial side of the leaf was always used. The plants were collected from outside (o) or grown under controlled conditions in a phytotron (p) or under controlled conditions in a greenhouse (g), as indicated.

The 8-s experiment

In the 8-s experiment we recorded the fluorescence fingerprints of seven plant species. The signal was measured from both sides of the leaf in three cases, and so we had 10 different classes of fingerprint curves. To record a fluorescence fingerprint curve, we took a leaf from the dark and illuminated it under the fluorometer, using four different light regimes (Fig. 2 *A*). The following fluorescence phases were recorded in the 8-s experiment: first a stable F_0 level, then a slight increase when the modulation frequency of the measuring beam was switched from 1.6 to 100 kHz, then an O-I-D-P-transient (see Fig. 1 for the definitions of these phases) when a red LED illuminator (moderate light) was switched on, and finally an increase to the F_{MAX} level when a high light flash was fired.

As expected, the general pattern of changes in the fluorescence signal was similar in all species studied (Fig. 2 *C*); only the curves of both conifers could be easily identified by eye. However, the pattern recognition procedure was able to recognize the species with almost 97% accuracy (Table 1), using only 16 numerical parameters extracted from each curve (Fig. 2 *B*). Interestingly, most mistakes in the 8-s experiment were made in mixing the upper and lower sides of birch and pea leaves.

The pattern recognition test was carried out with three different algorithms: BMD, 9-NN, and the MLP neural network method. The overall percentage of recognition was highest with the MLP method (96.6%; see Table 1), whereas the BMD method gave a recognition percentage of 81.3%, and the 9-NN method yielded 91.8% correct recognitions.

Table 6 shows that the misclassifications made by the 9-NN method were essentially a subset of the errors of the BMD method. The MLP was able to avoid most errors common to the BMD and 9-NN methods but made a small number of unique misclassifications. Voting between the results of the three classification methods and choosing the result of the MLP when all three methods disagree resulted in a slightly lower percentage of correct recognitions than using MLP alone (data not shown).

The 3-s experiment

We also tested 3-s-long fluorescence traces to gain insight into the effect of shortening the measurement time. The illumination phases of the 3-s curves (Fig. 2 *D*) were designed so that the fluorescence traces contained as large a

TABLE 3 Recognition matrix of the 3-s experiment, using BMD for the identification

	Recognized as									
Species	*Betula* (o)	*Nicotiana* (p)	*Zea* (p)	*Secale* (p)	*Secale* (g)	*Elytrigia* (g)	*Pinus* (o)	*Polytrichum* (o)	*Sphagnum* (o)	*Hylocomnium* (o)
Betula (o)	95	3	0	0	1	0	0	0	0	0
Nicotiana (p)	9	69	6	0	1	14	0	0	0	0
Zea (p)	3	8	81	5	2	0	0	0	0	0
Secale (p)	0	0	29	26	19	20	1	4	0	0
Secale (g)	0	0	0	0	69	29	0	1	0	0
Elytrigia (g)	0	0	0	9	12	78	0	0	0	0
Pinus (o)	0	0	0	0	0	0	94	5	0	0
Polytrichum (o)	0	0	0	0	0	0	0	88	10	1
Sphagnum (o)	0	0	0	0	1	0	0	15	82	1
Hylocomnium (o)	0	0	0	0	1	0	0	9	3	86

See the footnote of Table 2 for all other details of the experiments.

TABLE 4 Recognition matrix of the 3-s experiment, using a 9-NN algorithm for the identification

	Recognized as									
Species	*Betula* (o)	*Nicotiana* (p)	*Zea* (p)	*Secale* (p)	*Secale* (g)	*Elytrigia* (g)	*Pinus* (o)	*Polytrichum* (o)	*Sphagnum* (o)	*Hylocomnium* (o)
Betula (o)	95	3	0	0	0	0	0	0	0	1
Nicotiana (p)	3	95	1	0	0	0	0	0	0	0
Zea (p)	2	5	88	3	1	0	0	0	0	0
Secale (p)	0	3	16	63	9	5	0	3	0	0
Secale (g)	0	0	0	0	96	3	0	2	1	0
Elytrigia (g)	0	0	0	0	2	97	0	0	0	0
Pinus (o)	0	0	0	0	0	0	97	2	0	0
Polytrichum (o)	0	0	0	0	0	0	0	92	7	0
Sphagnum (o)	0	0	0	0	0	0	0	5	93	1
Hylocomnium (o)	0	0	0	0	1	0	0	10	0	88

See the footnote of Table 2 for all other details.

number of details as could be recorded, with a reasonable signal-to-noise ratio, with the PAM-103 fluorometer and its standard accessories (Fig. 2, *D* and *F*). As with the 8-s experiment, we extracted 16 features from each curve by calculating eight regression lines along the curve (Fig. 2 *E*).

The recognition matrices of the 3-s experiment (Tables 2–4) show that a high recognition accuracy (95.0%) could still be reached with these shorter measurements by using the MLP neural network. As also shown by the 8-s experiment, phylogenetically distant plants are easier to distinguish from each other than close relatives. The mixing of tobacco, phytotron rye, and maize (Table 2), all of which were grown in a phytotron under identical conditions, also reveals that an extreme uniformity in growth conditions induces a certain degree of similarity in the fluorescence responses of different species. The BMD and 9-NN methods in particular also mixed the signals of the two greenhouse-grown monocots, rye and coach grass (Tables 3 and 4).

Further shortening of the curve was then tested by using only 1-s fluorescence signals, obtained by cutting the 3-s curves before the pulse of saturating white light and using only the initial part of the data for the pattern recognition (Fig. 2 *F*). Even in this case, the MLP neural network was able to identify over 90% of the curves correctly (Table 5); the percentage of correct recognitions decreased considerably, however, when the BMD and 9-NN methods were used, as compared to the 3-s signal.

Patchiness in growth conditions of a field might be considered a problem when identifying plants from their fluorescence fingreprints. We mimicked patchiness by pooling data from birch, tobacco, and pine and then treating this combination as one species. These three species lie far from each other in the SOM (Fig. 4), and as expected, the BMD method classified members of this combination species randomly into several classes (recognition matrix not shown). However, the percentage of correct recognitions reached with the 9-NN and MLP neural network methods remained unchanged, although one of the classes was an extremely variable artificial class of three species (Table 5).

DISCUSSION

In addition to species-dependent differences in shape, plant species differ in physiology, and each species responds in its own way to environmental signals. We used chlorophyll fluorescence to reveal some species-dependent physiological responses and the method of pattern recognition to quantify these differences. The results suggest that chlorophyll fluorescence can be used, with a high accuracy, as a built-in "barcode" to identify plant species automatically.

The most powerful pattern recognition method of the present study was the MLP neural network. In this method, the teaching process can be carried out within minutes by using a modern standard PC, and the actual recognition takes a fraction of a second. The high recognition accuracy obtained with the large and independent test sets indicates that the learning process of the MLP network is successful, even with a moderate number of training cases.

The misclassifications (Table 6) are instructive from the practical point of view, because all three classifiers, MLP, BMD, and 9-NN, made mistakes that were unique to the classifier. Although little can be done to correct the common misclassifications, it may be possible to use several pattern recognition methods together to reduce the number of unique mistakes. Although simple voting between the three methods applied here did not yield better results than using

TABLE 5 Percentages of correct recognitions obtained from 8-s- and 3-s-long fluorescence traces and from the first 1 s of the 3-s experiment, analyzed by three different pattern recognition methods: MLP, BMD, and 9-NN

Length of curve (s)	Signal classes	Percentage of correct recognitions		
		MLP	BMD	9-NN
8	10	96.6	81.3	91.8
3	10	95.9	77.6	91.3
1	10	90.5	71.0	84.7
3	8	95.2	65.4	91.9

In the experiment with eight signal classes, one class was obtained by pooling *Betula*, *Nicotiana*, and *Pinus* signals.

TABLE 6 Misclassifications of the 3-s experiment, analyzed by three different pattern recognition methods: MLP, BMD, and 9-NN

Method	Mistakes unique to the method (%)	Mistakes common with MLP (%)	Mistakes common with BMD (%)	Mistakes common with 9-NN (%)	Mistakes common to all methods (%)
MLP	37	100	56	54	48
BMD	63	10	100	36	9
9-NN	5	26	92	100	22

The values are percentages of all misclassifications made by the method.

the MLP alone, the MLP may be used more efficiently, e.g., by using several different MLP networks and voting between the results or by estimating the goodness of the classification made by the MLP and using other classifiers if the result is vague. These types of more elaborate classification methods would require more computing time during the teaching period but would add little to the time spent on the actual recognition.

In addition to the differences between the fluorescence curves, two factors largely determine the success of plant identification. One is the design of the illumination process, and the other is the choice of the input parameters. The high recognition accuracy obtained in the 1-s experiment is especially promising because the intensity of the illumination used in this part of the fluorescence curve was fairly low. A better choice of the input parameters may further improve the accuracy of the identification.

The two sides of a leaf have large morphological differences at the cellular level, and the illumination conditions of the two sides are far from being similar. Because of the optical thickness of plant leaves, the fluorescence signal is dominated by the cell layers located nearest to the surface under study. It is therefore not surprising that the fluorescence fingerprint of the upper and lower sides of a leaf may differ almost as much as the fingerprints of two different species (Table 1). However, the finding that the upper and lower sides of birch leaves are easily mixed shows that some of the species-dependent features reflected by the fingerprint signal are present in all cell layers of the leaf. The same conclusion can be drawn from the pea data (Table 1).

The experiments in which signals from several plant species (Table 5) were pooled into an artificial "species" are especially promising because they suggest that fluorescence fingerprinting can be used for identifying groups of species or a single species growing in patchy growth conditions. It may actually be possible to identify two classes of plants on a certain field: weeds and cultivated plants.

The exact methods used in this study were not optimized for any particular use. For example, a very rapid method can undoubtedly be developed to identify gymnosperms from angiosperms, as the fluorescence fingerprints of these two groups already differ markedly during the very beginning of our fluorescence curves (Fig. 2, *C* and *F*). A large variety of additional optical treatments, e.g., responses to different light intensities, can easily be added to the identification protocol to increase the number of details in the fluorescence curves. The success of the 3-s and 1-s experiments (Tables 2–5) compared to the much longer 8-s curves (Table 1) demonstrates that a higher number of details in the curve leads to a better accuracy of the recognition. The power of details lies in the fact that on encountering a new detail every species faces a new opportunity to behave in a way that differs from the other species.

The number of features extracted from the curve can also be increased by utilizing the OIJP part of the Kautsky curve (Strasser et al., 1995) more efficiently, or by fitting some sections of the curve to higher order polynomials instead of calculating regression lines. Unfortunately the PAM fluorometer that we used is not suitable for the OJIP measurement in the submillisecond range. The use of the OJIP part of the data might also lead to development of a much faster method than the one we describe here.

The 8-s and 3-s curves contain a high-intensity pulse of white light (Fig. 2) that provides a natural scaling point. The F_{MAX} level may be difficult to reach within less than a few hundred milliseconds (Schreiber, 1986), even in high light. However, the success of the 1-s experiment (Table 5) shows that identification is possible even if F_{MAX} is not reached.

A possible application for fluorescence fingerprinting is a device that automatically detects the presence of a plant on a field, identifies the species, and informs a herbicide sprayer about the locations of weeds and cultivated plants. Although our laboratory experiments employed field-incompatible methods like long-lasting recording of fluorescence and a full darkening of the leaves before the measurement, we are confident that fluorescence fingerprinting can be utilized in automatic identification of plants in precision farming. Fluorescence fingerprints may also be applicable in diagnostics of complicated physiological responses like plant diseases.

This work was supported by the Academy of Finland. MK was supported by a fellowship from Kone foundation. The Centre for Scientific Computing (CSC) is thanked for permission to use their computing facilities.

REFERENCES

Aro, E. M., I. Virgin, and B. Andersson. 1993. Photoinhibition of photosystem II. Inactivation, protein damage and turnover. *Biochim. Biophys. Acta.* 1143:113–134.

Blackmore, S. 1994. Precision farming: an introduction. *Outlook Agriculture.* 23:275–280.

Chen, B., and D. M. Titterington. 1994. Neural networks: a review from a statistical perspective. *Stat. Sci.* 9:2–54.

Cohen, A. 1988. Biomedical Signal Processing, Vol. II, Compression and Automatic Recognition. CRC Press, Boca Raton, FL.

Fu, K. S. 1982. Syntactic Pattern Recognition and Applications. Prentice-Hall, Englewood Cliffs, NJ.

Govindjee. 1995. Sixty-three years since Kautsky: chlorophyll *a* fluorescence. *Aust. J. Plant Physiol.* 22:131–160.

Jain, A. K. 1988. Algorithms for Clustering Data. Prentice Hall, Englewood Cliffs, NJ.

Kautsky, H., and A. Hirsch. 1931. Neue Versuche zur Kohlensäureassimilation. *Naturwissenschaften.* 19:964.

Kohonen, T. 1990. The Self-Organizing Map. *Proc. IEEE.* 78:1464–1480.

Kohonen, T., J. Hynninen, J. Kangas, and J. Laaksonen. 1995. SOM-PAK, the Self-Organizing Map Program Package, Version 3.1. SOM Programming Team of the Helsinki University of Technology, Helsinki, Finland.

Krause, G. H., and E. Weis. 1991. Chlorophyll fluorescence and photosynthesis: the basics. *Annu. Rev. Plant Physiol. Plant Mol. Biol.* 42:313–349.

Lindgren, K., and J-E. Hällgren 1993. Cold acclimation of *Pinus contorta* and *Pinus sylvestris* assessed by chlorophyll fluorescence. *Tree Physiol.* 13:97–106.

Rich, E., and K. Knight. 1991. Artificial Intelligence, 2nd Ed. McGraw-Hill, Singapore.

Schalkoff, R. J. 1992. Pattern Recognition: Statistical, Structural and Neural Approaches. John Wiley and Sons, Singapore.

Schreiber, U. 1986. Detection of rapid induction kinetics with a new type of high frequency modulated chlorophyll fluorometer. *Photosynth. Res.* 9:261–272.

Schreiber, U., U. Schliwa, and W. Bilger. 1986. Continuous recording of photochemical and non-photochemical chlorophyll fluorescence quenching with a new type of modulation fluorometer. *Photosynth. Res.* 10:51–62.

Schreiber, U., W. Vidaver, V. C. Runeckles, and P. Rosen. 1978. Chlorophyll fluorescence assay for ozone injury in intact plants. *Plant Physiol.* 61:80–84.

Shaw, D. R., T. F. Peeper, and D. L. Notziger. 1985. Comparison of chlorophyll fluorescence and fresh weight as herbicide bioassay techniques. *Weed Sci.* 33:29–33.

Stirbet, A., Govindjee, B. J. Strasser, and R. J. Strasser. 1998. Chlorophyll *a* fluorescence induction in higher plants: modelling and numerical simulation. *J. Theor. Biol.* 193:131–151.

Strasser, R. J., A. Srivastava, and Govindjee. 1995. Polyphasic chlorophyll *a* fluorescence transient in plants and cyanobacteria. *Photochem. Photobiol.* 61:32–42.